

Molecular Weight Characterization of Conjugated Polymers through Gel Permeation Chromatography and Static Light Scattering

Ryan A. Fair¹, Renxuan Xie², Youngmin Lee³, Ralph H. Colby^{1,4}, and Enrique D. Gomez^{1,2,4}*

¹ Department of Materials Science and Engineering, The Pennsylvania State University, University Park, PA 16802

²Department of Chemical Engineering, The Pennsylvania State University, University Park, PA 16802

³Department of Chemical Engineering, New Mexico Institute of Mining and Technology, Socorro, NM 87801

⁴Materials Research Institute, The Pennsylvania State University, University Park, PA 16802

*Correspondence to edg12@psu.edu

Abstract

Molecular weight is a key parameter of any polymer. Characterizing the molecular weight of conjugated polymers is often non-trivial due to their semiflexible backbones and poor solubilities. Perhaps the most used technique for measuring molecular weight is gel permeation chromatography (GPC), and results are often calibrated relative to flexible polymer standards. This mismatch between chain flexibilities of samples and standards, combined with poor sample solubility in the mobile phase, leads to inaccuracies in many GPC measurements of conjugated polymers. In this work, we use a universal calibration combined with in-line concentration measurements to yield reliably accurate results for polymers of various stiffnesses. Accuracy of results are verified with absolute molecular weights obtained from static light scattering (SLS). We show that measuring the refractive index increment is key to confirm full recovery of the polymer and ensure accurate values of the absolute molecular weight from GPC.

Keywords: Gel Permeation Chromatography, Intrinsic Viscosity, Static Light Scattering, Conjugated Polymers, Refractive Index Increment

Introduction

The molecular weight of polymers can affect crystallinity¹, solubility², phase transition temperatures^{3, 4}, and morphology^{4, 5}. These, in turn, significantly affect mechanical, electrical, thermal, and optical properties, and thereby set suitable processing conditions for various applications. There are various methods to characterize the molecular weight and molecular weight distribution of polymers, such as resolving chains of different molecular weights through matrix-assisted laser induced spectroscopy and resolving differences in retention time in Gel Permeation Chromatography (GPC). GPC in particular is applicable to a wide range of molecular weights, making it a widely-used technique⁶.

GPC detectors can measure the refractive index, light scattering, viscosity and optical absorption at various wavelengths, among other parameters. These detectors measure the retention time (t_r) of dissolved polymers as they pass through permeable columns. t_r is then, to first order, inversely correlated to a coil size, or radius of gyration (R_g), in solution. A simple approach to relate t_r with molecular weight uses a polymer, such as polystyrene (PS), with known molecular weight as a reference⁷. R_g is then assumed to consistently correlate with the molecular weight of the chain. Thus, an inherent assumption of using a polymer standard for GPC analysis is that the persistence length (l_p) of the test polymer is equivalent to that of the reference polymer (e.g., PS), and that the chain swelling in the carrier solvent is also the same between the test and reference polymer.

Conjugated polymers are significantly stiffer than polystyrene ($l_p \sim 1$ nm)^{8,9}. For example, poly(3-hexylthiophene-2,5-diyl) has an l_p of 2.8 nm, and polydioctylfluorene (PFO) has an l_p of

7.0 nm¹⁰. The degree of swelling of these chains in solvents used for GPC (for example, tetrahydrofuran, chloroform, chlorobenzene, and 1,2,4-trichlorobenzene) is currently underexplored. Thus, estimates of the molecular weight of semiflexible polymers from GPC measurements that are calibrated against polystyrene are not likely to be accurate¹¹.

A universal calibration for GPC data was proposed by Benoit using measurements of the intrinsic viscosity ($[\eta]$)¹². The product of the intrinsic viscosity and molecular weight, $[\eta]M$, is directly proportional to the hydrodynamic volume, which is correlated with the retention volume for any polymer. Once a reference polymer is measured, the molecular weight for any polymer can be obtained from the intrinsic viscosity so long as separation within the column is ideal and governed only by entropic effects as the polymer explores the pores, and not non-ideal interactions between the polymer and column. For polymers with similar topology, the intrinsic viscosity can also be related to M with the Mark-Houwink equation, as $[\eta] = kM^\alpha$, where k and α are constants that depend on the specific polymer-solvent system¹³.

Previous work on conjugated polymers has demonstrated good agreement between PS-relative molecular weights from GPC and molecular weights from other techniques, such as static light scattering (SLS)^{14, 15}. Others have illustrated the expected disagreement between PS-relative molecular weights from GPC compared with molecular weights from viscometry¹⁶, matrix-assisted laser deposition/ionization (MALDI)¹⁷, and end-group analysis of nuclear magnetic resonance (NMR) spectra^{18, 19}. Nevertheless, the use of a universal calibration for GPC traces to extract the absolute molecular weight of conjugated polymers remains largely unexplored, with few exceptions²⁰.

Here, we demonstrate the importance of measuring the refractive index increment, dn/dc , to measure the amount of polymer exiting the columns and thereby identify whether any material

is lost during the measurement²¹. Furthermore, we show that PS swells more than some conjugated polymers in the carrier solvent, chlorobenzene²², and leads to a fortuitous agreement between accurate molecular weights and PS-relative calibrations. As such, this work proposes an explanation of the intermittent success of molecular weight determination of conjugated polymers from GPC using PS standards, while also establishing procedures for extracting absolute molecular weights using a universal calibration.

Materials and methods

The lowest molecular weight P3HT was synthesized using Kumada coupling²³, while all other batches were purchased from Millipore Sigma. An argon-purged reactor was filled with 5 mL of anhydrous tetrahydrofuran (THF) and monomer, 2,5-dibromo-3-hexylthiophene, before a 0.95 molar ratio of the Grignard reagent, 1.4 M isopropyl magnesium chloride in THF, was added dropwise. The mixture reacted for 3 hours and then the reactor was charged with an additional 30 mL of THF and a 0.015 molar ratio of catalyst, 1,3-bis(diphenylphosphino)propane nickel(II) chloride, and allowed to react for another 20 minutes. The reaction was then terminated with 2 mL of 5 M HCl, leaving a hydrogen end group. The reaction mixture was then precipitated overnight in 500 mL of methanol before being filtered. Polymer product was purified using Soxhlet extraction in methanol and acetone for 8 to 12 hours in each solvent. PFO samples were purchased from Ossila. PS calibrants were purchased from Agilent. All other materials and reactants were purchased from Millipore Sigma.

Gel permeation chromatography samples were prepared in chlorobenzene at concentrations of 1.0 mg/mL or 0.5 mg/mL depending on solubility. Before running them, samples were stirred overnight at 40°C. Samples were run through an Agilent 1260 Infinity system outfitted with four silica gel columns in series, two ResiPore guard columns, a ResiPore 300 x 7.5 mm column, and

a PLgel 10 μm MIXED-B 300 x 7.5 mm column. The chlorobenzene mobile phase passed through a degasser at a constant flowrate of 0.5 mL/min before the sample was injected into the stream using a sample autoloader. Column temperature was maintained at 40°C. A 640 nm inline differential refractive index detector and four-capillary fused silica bridge viscometer, both contained within the Agilent 1260 Infinity multi-detector suite, were used to measure elution profiles. The viscometer was used for universal calibration measurements while the refractive index signal was used to calculate percent recovery using a known value of refractive index increment (dn/dc). Molecular weights were calculated using PS standards and using a universal calibration by measuring the product of intrinsic viscosity and retention time.

A Brookhaven BI-DNDC deflection-type refractometer was used to measure dn/dc for each polymer at 40°C in chlorobenzene with a 620 nm laser. Samples were mixed overnight at 40°C. Red lasers were selected for these experiments as the wavelengths are outside the absorption range of all the materials used^{24, 25}. Polymer solutions were prepared at five concentrations to measure refractive index as a function of concentration. These ranged from 1.0 mg/mL to 5.0 mg/mL, and were injected starting at the lowest concentration and working upwards.

Static light scattering measurements were carried out using a Brookhaven BI-APDX photon detector and BI-200SM goniometer with a 640 nm Brookhaven laser at 10 mV. Exposure time was fixed at 1 second with a dust rejection ratio of 1.33. Ten measurements within tolerance were expected before the average was accepted, with a maximum of 100 measurements taken. Pure chlorobenzene scattering was measured at 40°C and angles ranging from 30° to 130° at intervals of 5° before polymer solution scattering was measured. Polymers were dissolved overnight in chlorobenzene at 40°C and were measured starting at concentrations as high as 5.0 mg/mL. This solution was diluted in the same test tube for sequential measurements at lower concentrations,

working down until at least six concentrations were measured, often going as low as 0.5 mg/mL depending on signal-to-noise ratio. The data was then used to construct Zimm plots and calculate M_w and R_g for each polymer using software from Brookhaven.

Intrinsic viscosities of P3HT in chlorobenzene were recorded using an Ubbelohde viscometer at 40.0°C. A cup and bob geometry was used at steady shear with a shear rate varying from 1 s⁻¹ to 100 s⁻¹ in a stress-controlled experiment. Samples were dissolved overnight at 40°C. These measurements were used for constructing a Mark-Houwink plot.

Results and discussion

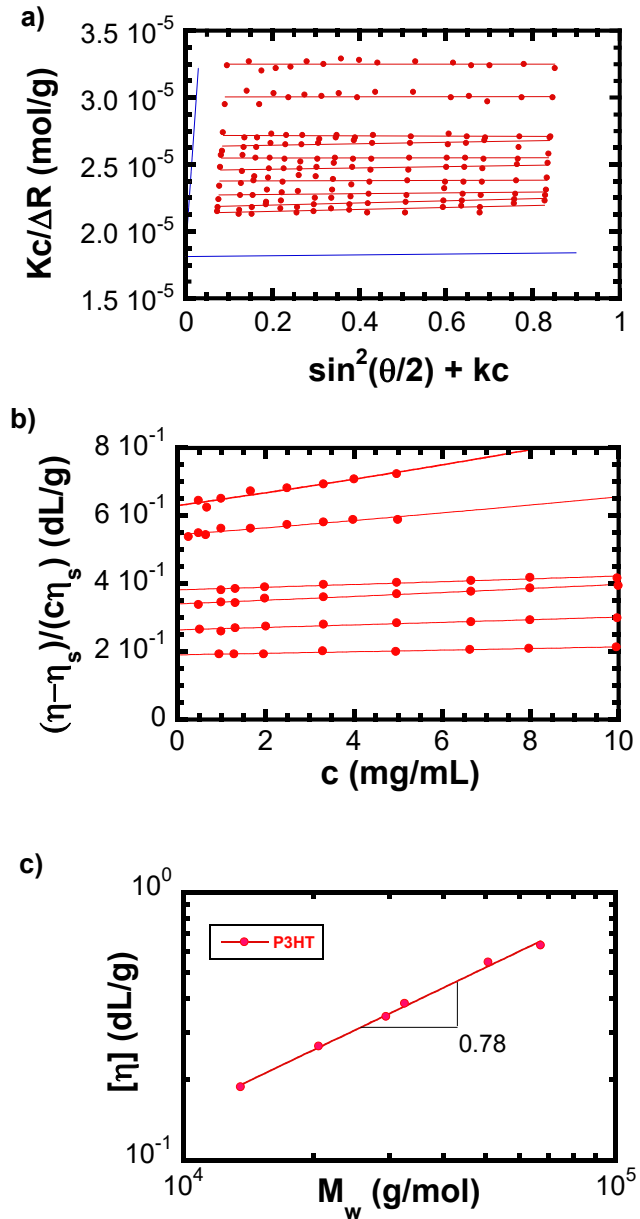


Figure 1: (a) Zimm plot of P3HT ($M_w = 54.8$ kDa) dissolved in chlorobenzene at 40°C from SLS. The red points are intensities measured at various angles and concentrations, as detailed in the methods section. The red lines are linear fits to the data, and the blue lines are extrapolations to zero scattering angle (nearly vertical line) and zero concentration (nearly horizontal line). (b) Huggins plot for six P3HT samples dissolved in chlorobenzene at 40.0°C. (c) Mark-Houwink plot of P3HT dissolved in chlorobenzene at 40.0°C. Line is a power-law fit to the data that leads to $[\eta] = (1.23 * 10^{-4}) * M_w^{0.78}$.

We obtained the absolute weight-average molecular weight of P3HT and PFO using Zimm plots generated from static light scattering, and we later compare these values to results from GPC. A representative example is shown in Fig. 1a. The Zimm plot shows the concentration (c) and angular (θ) dependences of the reciprocal Rayleigh ratio (ΔR), normalized by concentration and the optical constant K . K is given by $\frac{4\pi^2 n^2 \left(\frac{dn}{dc}\right)^2}{\lambda^4 N_{Av}}$, which gives a value of 2.76×10^{-13} for refractive index n of 1.524 (chlorobenzene) and $dn/dc = 0.1550$ mL/g for P3HT in chlorobenzene at a wavelength λ of 640 nm (N_{Av} is Avogadro's number). dn/dc was measured as described below. As shown in Figure 1a, the weight-average molecular weight (M_w) can be readily extracted from the intercept as both angle and concentration are extrapolated to zero, the second virial coefficient (A_2) is obtained from the slope of the zero-angle extrapolation line (nearly vertical blue line in Fig. 1a), and the radius of gyration (R_g) is obtained from the slope of the zero-concentration extrapolation line (nearly horizontal blue line in Fig. 1a). For data from regioregular P3HT shown in Fig. 1a, we obtain a weight-average molecular weight M_w of 54.8 kDa and a z-average radius of gyration R_g of 12.2 nm.

This R_g implies a persistence length of 3.7 nm based on the Kratky-Porod model for a worm-like chain under theta solvent conditions²⁶ shown in equation 1:

$$\frac{\langle R_g^2 \rangle}{(2l_p)^2} = \frac{n_K}{6} - \frac{1}{4} + \frac{1}{4n_K} - \frac{1-e^{-2n_K}}{8n_K^2} \quad (1)$$

l_0 is the length of a monomer, M_0 is the molecular weight of a monomer, and n_K is the number of Kuhn segments along the polymer backbone. This persistence length is a little larger than most previously reported values²⁷, including previous computational predictions (4.0 nm²⁸ or 2.8 nm²⁹),

neutron scattering data (3.0 nm^{30}), and light scattering results (2.4 nm^1). As we discuss below, this implies chlorobenzene is a good solvent for P3HT such that chains are swollen.

Having established values for absolute molecular weights, we verify that the Mark-Houwink equation accurately describes the intrinsic viscosity of our polymers. Intrinsic viscosity measurements were performed in solution at various concentrations. The results are shown as a Huggins plot in Figure 1b. The intercept of the power law fit provides the intrinsic viscosity. As shown in Figure 1c, the intrinsic viscosity of P3HT dissolved in chlorobenzene follows a power law of the form

$$[\eta] = (1.23 * 10^{-4}) * M^{0.78} \quad (2)$$

This exponent of 0.78 is consistent with chlorobenzene being a good solvent (an exponent of 0.76 is expected)¹¹ for P3HT. In addition, this exponent is similar to what is obtained for polystyrene in chloroform (0.76) and chlorobenzene (0.749)³¹.

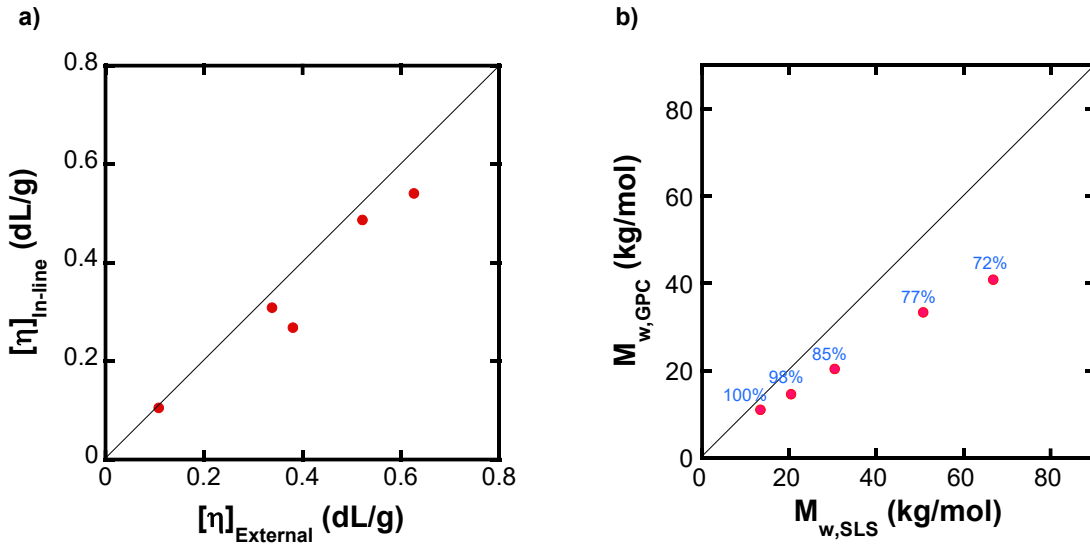


Figure 2: (a) Intrinsic viscosity of P3HT dissolved in chlorobenzene at 40°C measured using an external viscometer (x-axis) and the in-line viscometer on the GPC (y-axis). (b) Molecular weight obtained from GPC with a universal calibration ($M_{w,\text{GPC}}$) versus molecular weight obtained from SLS ($M_{w,\text{SLS}}$) for P3HT. All samples on this figure were run at a concentration of 1 mg/mL. The failure of GPC to accurately measure the molecular weight is observed when sample recovery is low (% recovery shown in blue above each point), such that molecular weights from GPC are underestimated. Lines are guide to the eye ($y = x$).

Having established that the intrinsic viscosity of P3HT follows the Mark-Houwink equation, we employ a combination of a refractive index detector and in-line viscometer to yield an absolute molecular weight from GPC. The in-line viscometer was used for intrinsic viscosity measurements to construct the universal calibration. Figure 2a contrasts the intrinsic viscosities produced by the external viscometer with those from the in-line detector on the GPC. Figure 2b compares the molecular weight obtained from SLS to that obtained from GPC with a universal calibration using a 1 mg/mL concentration for all samples. The lowest molecular weight P3HT sample shows agreement between the M_w obtained from GPC and SLS, but as molecular weight increases, progressively less of the sample elutes from the columns (percent recovery decreases), causing an underestimation of M_w that gets worse as molecular weight increases, likely due to longer chains preferentially adsorbing to the columns³²⁻³⁴ and not eluting with the rest of the distribution.

The error in M_w values obtained from GPC could be due to interactions between the polymer and column causing some material to be trapped within the instrument, especially if sample loss is not uniform throughout the polymer molecular weight distribution. To quantify the amount of material lost, we use the inline differential refractive index detector to calculate the concentration of polymer exiting the columns assuming a constant value of dn/dc . Because limited values for dn/dc of these polymers are currently reported, we measured dn/dc , as shown in Figure 3a for P3HT in chlorobenzene. We show dn/dc values for polystyrene, poly(3-hexylthiophene-2,5-diyl), and polydioctylfluorene in chlorobenzene at 40 °C in Table 1. The values reported in this work agree with previous reports for similar polymers under different conditions^{14, 15, 20, 35, 36}. With a known dn/dc , we can calculate the percent recovery of polymer that is detected with the in-line differential refractive index detector in the GPC. The values for P3HT in chlorobenzene at 40 °C are shown in Figure 2b, as values next to the corresponding data points. As the molecular weight of P3HT increases, the percent recovery drops, and GPC underestimates the molecular weight. Thus, combining an inline differential refractive index detector with known dn/dc allows us to observe a correlation between underestimates of the molecular weight from GPC with percent recovery out of the columns.

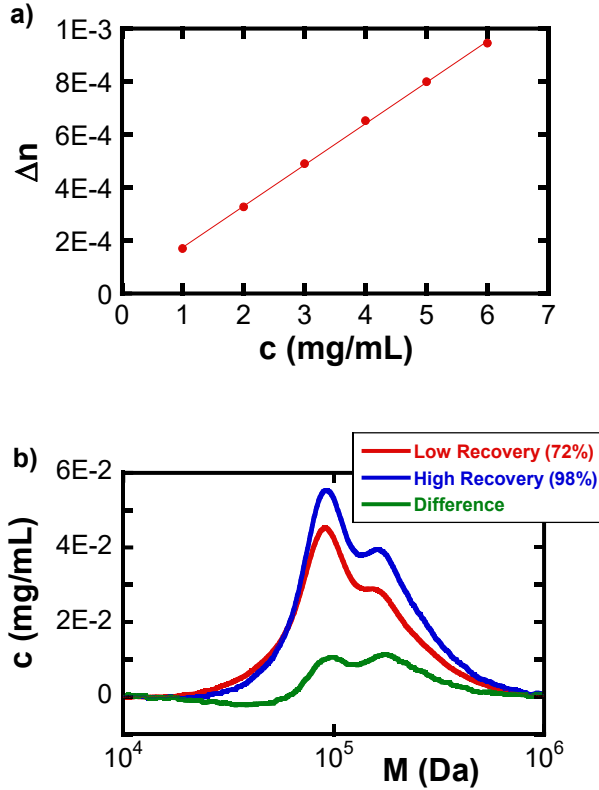


Figure 3: (a) Refractive index increment measurement of P3HT ($M_w = 65$ kg/mol from SLS) in chlorobenzene at 40°C. Linear fit represented by solid line. (b) GPC elution profiles of high molecular weight P3HT ($M_w = 94$ kg/mol from SLS) at low recovery (1.0 mg/mL in red) and high recovery (0.5 mg/mL in blue). Percent recovery is shown in the legend. The difference (green) shows the molecular weight distribution that fails to elute from the columns at 1.0 mg/mL.

Table 1: dn/dc values for polystyrene, P3HT, and PFO measured in chlorobenzene at 40°C with a wavelength of 640 nm.

Polymer*	dn/dc (mL/g)
Polystyrene ($M_w = 110$ kg/mol)	0.0866
Poly(3-hexylthiophene-2,5-diyl) ($M_w = 60$ kg/mol)	0.1550
Polydioctylfluorene ($M_w = 63$ kg/mol)	0.1130

* M_w determined from SLS.

Figure 3b shows the chromatography traces for P3HT ($M_w = 67.0$ kg/mol from SLS) at 1.0 mg/mL and 0.5 mg/mL, which have material recoveries of 72% and 98%, respectively. Calculating the difference as a function of molecular weight reveals a non-uniform loss for runs with lower recovery. This non-uniform sample loss, where higher molecular weight chains are

preferentially lost during the experiment, leads to underestimation of the weight-average molecular weight. Multiple sequential runs of high molecular weight samples consistently resulted in poor measured recovery; we thus surmise that the highest molecular weight fractions were not retained permanently within the column. Permanent retention within the columns might lead to saturation, such that subsequent runs would exhibit an increase in recovery. Rather, the high molecular weight fractions were likely eluting at small concentrations over longer time scales.

Lowering the concentration will decrease polymer adsorption³². Indeed, running samples at a lower concentration (0.5 mg/mL) leads to near 100% polymer recovery. As such, conditions are closer to ideal entropic separations. Figure 4a summarizes molecular weights from GPC (using a universal calibration) when nearly 100% of material was recovered, compared against molecular weights obtained from static light scattering. Two polymers with different batches that vary in molecular weight are shown, P3HT and PFO. The agreement between techniques is quantitative. Molecular weights and dispersities from GPC, as well as regioregularity for P3HT obtained from ¹H NMR as previously reported^{37, 38}, are shown in Table 2.

Table 2: Molecular weight (M_w), dispersity (D), concentration during GPC experiment (c_{GPC}), regioregularity (%RR), radius of gyration (R_g), 2nd virial coefficient (A_2), intrinsic viscosity [η], and Huggins coefficient (k_h) for polymers used in this study

Polymer	M_w (kg/mol) ^a	D ^{b*}	c_{GPC} (mg/mL)	%RR ^c	R_g (nm) ^a	$A_2 \times 10^4$ (cm ³ mol/g ²) ^a	$[\eta] \times 10^2$ (dL/g) ^d	k_h
P3HT	7.0	1.16	1.0	93.0%	-	97.8 ± 9.2	-	-
P3HT	13.6	-	-	-	-	-	1.88	0.654
P3HT	20.6	-	-	-	-	-	2.66	0.523
P3HT	29.5	1.60 ± 0.53	1.0	94.7%	-	-	3.43	0.484
P3HT	32.5	-	-	-	-	-	3.84	0.278
P3HT	38.3	1.60 ± 0.31	0.5	95.3%	-	40.7 ± 0.4	-	-
P3HT	50.8	-	-	-	-	-	5.48	0.353
P3HT	54.8	1.55 ± 0.41	0.5	95.7%	12.2 ± 2.4	23.0 ± 0.4	-	-
P3HT	58.6	-	-	-	12.2 ± 3.0	-	-	-
P3HT	67.0	1.70 ± 0.05	0.5	95.5%	-	19.4 ± 0.4	6.34	0.488
P3HT	70.8	1.56 ± 0.45	0.5	90.0%	15.7 ± 2.1	-	-	-
P3HT	98.1	-	-	-	17.4 ± 0.6	-	-	-
P3HT	109.0	-	-	-	17.5 ± 1.6	-	-	-
PFO	14.4	2.14 ± 0.15	1.0	-	-	18.6 ± 1.8	-	-
PFO	62.6	2.53 ± 0.34	0.5	-	13.3 ± 2.2	-	-	-

^aFrom SLS. ^bD from GPC. ^cRegioregularity from ¹H NMR. ^dIntrinsic viscosity from external viscometer.

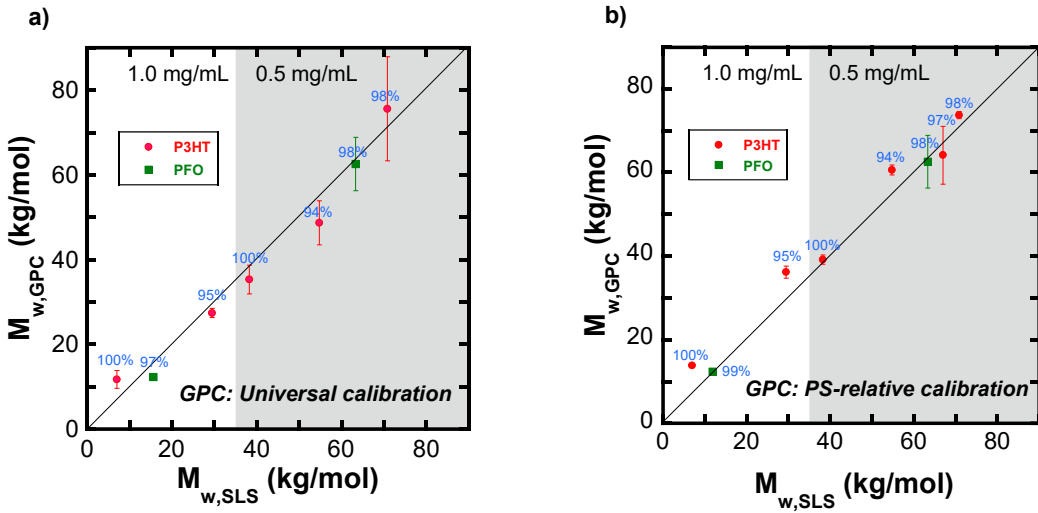


Figure 4. (a) Weight-average molecular weight from GPC using a universal calibration versus weight-average molecular weight from SLS. (b) PS-relative calibration versus weight-average molecular weight from SLS. Percent recovery is shown above each sample. Concentrations used for GPC experiments are denoted by white regions (1.0 mg/mL) and gray regions (0.5 mg/mL). Lines are guide to the eye ($y = x$).

In Figure 4b, we show molecular weights obtained from a PS-relative calibration while ensuring full sample recovery. In this approach, we relate the retention time of polystyrene chains eluting in chlorobenzene to the molecular weight of polystyrene standards. Test polymers are then assumed to elute in a similar manner as a function of molecular weight; this assumes a similar coil size as a function of molecular weight as polystyrene. Nevertheless, the agreement between SLS and GPC using a PS-relative calibration is again good for P3HT. This would be unexpected if we consider that l_p varies significantly between PS, P3HT, and PFO (1.0 nm^{8,9}, 2.8 nm¹⁰, and 7.0-8.6 nm¹⁰, respectively), such that R_g depends differently on M_w .

Using the persistence lengths, we predict the expected R_g for the various polymers under the assumption of theta solvent conditions for simplicity. The Kratky-Porod model for a wormlike chain in theta solvent conditions²⁶ is used for P3HT and PFO (equation 1). We assume an ideal linear chain for PS and thus use equation 3 to relate R_g , M , and l_p ³⁹:

$$\langle R_g^2 \rangle = \frac{l_p l_0 M}{3 M_0} \quad (3)$$

where M is the polymer molecular weight and l_0 and M_0 are defined as in equation 1. Given that chlorobenzene is a good solvent for PS and P3HT, we expect equations 1 and 3 to underestimate R_g for these polymers.

Dotted lines in Figure 5 show the expected R_g in a theta solvent (we use persistence lengths for PS, P3HT, and PFO of 1.0 nm^{8, 9}, 2.8 nm¹⁰, and 10.9 nm¹⁰), and points show R_g measured in chlorobenzene using SLS. Comparing these values reveals that PS and P3HT chains are swollen while PFO chains are collapsed, leading to fortuitously similar R_g for all polymers when dissolved in chlorobenzene at 40°C for a given molecular weight. The Mark-Houwink exponent (α) provides another point of comparison between P3HT (0.78) and PS (0.749)³¹. The similar good solvent conditions that these values indicate mean that both polymers are behaving as random coils. The observed swelling and contraction effects are likely due to the non-theta solvent conditions for the polymers in this study; chlorobenzene is a good solvent for PS and P3HT, but it is a poor solvent for PFO. The kinetics of PFO chain collapse in these sub-theta conditions may be preempting the kinetics of chain aggregation on the time scales observed, leading to the small observed radius. Such a phenomenon has been previously observed in other poor solvent systems⁴⁰⁻⁴².

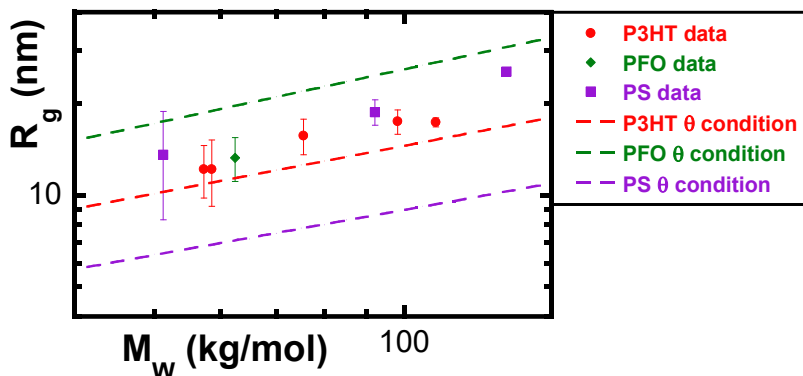


Figure 5. Radius of gyration (R_g) versus weight-average molecular weight for PS, P3HT, and PFO in chlorobenzene measured from SLS (points, data) and expected assuming theta solvent conditions (θ condition).

The non-theta conditions for the systems used here fortuitously lead to similar coil sizes in solution⁴³⁻⁴⁵. This results in similar retention times for polymers with similar molecular weights regardless of differences in persistence length. We speculate that the likelihood of other conjugated polymers also exhibiting similar coil sizes in solution as PS is not high^{30, 46, 47}. Nevertheless, our work provides a possible explanation for why some reports demonstrate accurate estimates of the molecular weight of conjugated polymers from GPC with a PS calibration while others do not.

Summary and conclusions

Coil sizes of chains with equivalent molecular weights will be significantly different if their persistence lengths are sufficiently disparate, as is the case between PS and semiflexible conjugated polymers. Therefore, GPC calibrations relative to PS standards should not, in principle, produce accurate results for semiflexible polymers. This work proposes an explanation for why GPC with PS standard calibrations produce accurate results in some cases, while in other instances the results are inaccurate. If chains are short, they are less likely to adsorb to columns, but as chains get longer more and more adsorbs to the column, leading to underestimates of molecular weight.

Based on the conditions of the system, especially the mobile phase, polymer-column interactions could be weak enough to prevent polymer adsorption, otherwise the tendency of longer chains to preferentially adsorb leads to unreliable measures of the molecular weight of semiflexible polymers.

We can confirm minimal polymer adsorption using a refractive index increment measurement to allow for determining the exiting polymer concentration and therefore the precent polymer recovery. Any polymer loss must be addressed through concentration reduction, adjusting the temperature, and changes in the carrier solvent, for example with salts, to increase solubility and prevent polymer adsorption to the columns^{14, 15}. Having established nearly 100% recovery, we have shown that a universal calibration for the GPC that relies on measuring the viscosity and refractive index can yield accurate molecular weights for semiflexible polymers, as verified by static light scattering measurements.

Acknowledgements

Funding support from the National Science Foundation under award number DMR-1921854 is gratefully acknowledged.

References

1. Heffner, G. W.; Dahman, S. J.; Pearson, D. S.; Gettinger, C. L., The effect of molecular weight and crystallinity on the conductivity of a conducting polymer. *Polymer* **1993**, *34*, 3155-3159.
2. de Castro Macêdo Fonsêca, J.; dos Prazeres Arruda da Silva Alves, M., Influence of solvent used on oxidative polymerization of Poly(3-hexylthiophene) in their chemical properties. *Polímeros* **2018**, *28*, 395-399.
3. Xie, R.; Lee, Y.; Aplan, M. P.; Caggiano, N. J.; Müller, C.; Colby, R. H.; Gomez, E. D., Glass Transition Temperature of Conjugated Polymers by Oscillatory Shear Rheometry. *Macromolecules* **2017**, *50*, 5146-5154.
4. Xie, R.; Aplan, M. P.; Caggiano, N. J.; Weisen, A. R.; Su, T.; Müller, C.; Segad, M.; Colby, R. H.; Gomez, E. D., Local Chain Alignment via Nematic Ordering Reduces Chain Entanglement in Conjugated Polymers. *Macromolecules* **2018**, *51*, 10271-10284.
5. Kline, R. J.; McGehee, M. D.; Kadnikova, E. N.; Liu, J.; Fréchet, J. M. J.; Toney, M. F., Dependence of regioregular poly(3-hexylthiophene) film morphology and field-effect mobility on molecular weight. *Macromolecules* **2005**, *38*, 3312-3319.
6. Striegel, A. M.; Yau, W. W.; Kirkland, J. J.; Bly, D. D., Modern Size-Exclusion Liquid Chromatography. **2009**, *399* (4), 1571-1572.
7. Giddings, J. C.; Mallik, K. L., Theory of Gel Filtration (Permeation) Chromatography. *Analytical Chemistry* **1966**, *38*, 997-1000.
8. Wignall, G. D.; Ballard, D. G. H.; Schelten, J., Measurements of persistence length and temperature dependence of the radius of gyration in bulk atactic polystyrene. *European Polymer Journal* **1974**, *10*, 861-865.
9. Ding, Y.; Sokolov, A. P., Comment on the dynamic bead size and Kuhn segment length in polymers: Example of polystyrene. *Journal of Polymer Science, Part B: Polymer Physics* **2004**, *42*, 3505-3511.
10. Kuei, B.; Gomez, E. D., Chain conformations and phase behavior of conjugated polymers. *Soft Matter* **2017**, *13*, 49-67.
11. Rubinstein, M.; Colby, R. H., *Polymer Physics*. Oxford University Press: 2003.
12. Grubisic, Z.; Rempp, P. F.; Benoit, H. C., A universal calibration for gel permeation chromatography. *Journal of Polymer Science Part B: Polymer Letters* **1967**, *5*, 753-759.
13. Striegel, A. M., Viscometric Detection in Size-Exclusion Chromatography: Principles and Select Applications. *Chromatographia* **2016**, *79*, 945-960.
14. Heffner, G. W.; Pearson, D. S., Molecular Characterization of Poly(3-hexylthiophene). *Macromolecules* **1991**, 6295-6299.

15. Heffner, G. W.; Pearson, D. S., Characterization of Poly(3-Octylthiophene). 1: Molecular Characterization in Dilute Solution. *Polymer Engineering and Science* **1995**, *35*, 860-867.

16. Holdcroft, S., Determination of molecular weights and Mark–Houwink constants for soluble electronically conducting polymers. *Journal of Polymer Science Part B: Polymer Physics* **1991**, *29*, 1585-1588.

17. Liu, J.; Loewe, R. S.; McCullough, R. D., Employing MALDI-MS on poly(alkylthiophenes): Analysis of molecular weights, molecular weight distributions, end-group structures, and end-group modifications. *Macromolecules* **1999**, *32*, 5777-5785.

18. Wong, M.; Hollinger, J.; Kozycz, L. M.; McCormick, T. M.; Lu, Y.; Burns, D. C.; Seferos, D. S., An apparent size-exclusion quantification limit reveals a molecular weight limit in the synthesis of externally initiated polythiophenes. *ACS Macro Letters* **2012**, *1*, 1266-1269.

19. Gu, K.; Onorato, J.; Xiao, S. S.; Luscombe, C. K.; Loo, Y.-L., Determination of the Molecular Weight of Conjugated Polymers with Diffusion-Ordered NMR Spectroscopy. *Chemistry of Materials* **2018**, *30* (3), 570-576.

20. Konas, M.; Moy, T. M.; Shultz, R. A. R.; Ward, T. C., Molecular Weight Characterization of Soluble High Performance Polyimides. 2. Validity of Universal SEC Calibration and Absolute Molecular Weight Calculation. *Journal of Polymer Science: Part B: Polymer Physics* **1995**, *33*, 1441-1448.

21. Cheng, X. P.; Zhang, H. B.; Hu, J. J.; Feng, L. F.; Gu, X. P.; Jean-Pierre, C., Characterization of broad molecular weight distribution polyethylene with multi-detection gel permeation chromatography. *Polymer Testing* **2018**, *67*, 213-217.

22. Müller-Plathe, F., Local structure and dynamics in solvent-swollen polymers. *Macromolecules* **1996**, *29*, 4782-4791.

23. Lee, Y.; Aplan, M. P.; Seibers, Z. D.; Kilbey, S. M.; Wang, Q.; Gomez, E. D., Tuning the synthesis of fully conjugated block copolymers to minimize architectural heterogeneity. *Journal of Materials Chemistry A* **2017**, *5* (38), 20412-20421.

24. Park, Y. D.; Lee, S. G.; Lee, H. S.; Kwak, D.; Lee, D. H.; Cho, K., Solubility-driven polythiophene nanowires and their electrical characteristics. *J. Mater. Chem.* **2011**, *21*, 2338-2343.

25. Zhang, H.; Huang, L.; Li, T.; Liu, B.; Bai, Z.; Li, X.; Lu, D., Quantitative Structure-property Relationship of Polyfluorene Conjugated Polymers Condensed State from Solution to Film. *Acta Chimica Sinica* **2019**, *77*, 397-405.

26. Benoit, H.; Doty, P., Light Scattering from Non-Gaussian Chains. *J. Phys. Chem.* **1953**, *57* (9), 958-963.

27. Kuei, B.; Gomez, E. D., Chain conformations and phase behavior of conjugated polymers. *Soft Matter* **2017**, *13* (1), 49-67.

28. Zhang, W.; Gomez, E. D.; Milner, S. T., Predicting Chain Dimensions of Semiflexible Polymers from Dihedral Potentials. *Macromolecules* **2014**, *47* (18), 6453-6461.

29. Zhang, W.; Gomez, E. D.; Milner, S. T., Predicting Nematic Phases of Semiflexible Polymers. *Macromolecules* **2015**, *48* (5), 1454-1462.

30. McCulloch, B.; Ho, V.; Hoarfrost, M.; Stanley, C.; Do, C.; Heller, W. T.; Segalman, R. A., Polymer chain shape of poly(3-alkylthiophenes) in solution using small-angle neutron scattering. *Macromolecules* **2013**, *46*, 1899-1907.

31. Polymer Data Handbook, 2nd ed. *Polymer Data Handbook*, 2nd ed . Edited by James E. Mark (University of Cincinnati, OH). Oxford University Press: New York. 2009 . xii + 1250 pp. \$195.00. ISBN 978-0-19-518101-2 . *J. Am. Chem. Soc.* **2009**, *131*, 16330-16330.

32. de Gennes, P. G., Scaling theory of polymer adsorption. *Journal de Physique* **1976**, *37* (12), 1445-1452.

33. de Gennes, P. G.; Pincus, P., Scaling Theory of Polymer Adsorption: Proximal Exponent. *Journal de physique. Lettres* **1983**, *44*, 241-246.

34. Netz, R. R.; Andelman, D., Neutral and charged polymers at interfaces. *Physics Reports* **2003**, *380*, 1-95.

35. Temyanko, E.; Russo, P. S.; Ricks, H., Study of rodlike homopolypeptides by gel permeation chromatography with light scattering detection: Validity of universal calibration and stiffness assessment. *Macromolecules* **2001**, *34* (4), 582-586.

36. Badley, J. H., Estimation of Z-average molecular weight by light scattering in good solvents. *Journal of Polymer Science Part C: Polymer Symposia* **1965**, *8* (1), 305-312.

37. Smith, B. H. Enhanced charge transport in polymer thin-film transistors through structural and morphological optimization. 2016.

38. Kim, J.-S.; Kim, Y.; Kim, H.-J.; Kim, H. J.; Yang, H.; Jung, Y. S.; Stein, G. E.; Kim, B. J., Regioregularity-Driven Morphological Transition of Poly(3-hexylthiophene)-Based Block Copolymers. *Macromolecules* **2017**, *50* (5), 1902-1908.

39. Heimenz, P. C.; Lodge, T. P., *Polymer Chemistry*. Second ed.; CRC Press: 2007.

40. Maki, Y.; Sasaki, N.; Nakata, M., Coil-globule transition of poly(methyl methacrylate) in acetonitrile. *Macromolecules* **2004**, *37*, 5703-5709.

41. Maki, Y.; Dobashi, T.; Nakata, M., Kinetics of chain collapse in dilute polymer solutions: Molecular weight and solvent dependences. *Journal of Chemical Physics* **2007**, *126*.

42. Maki, Y., Chain collapse and aggregation in dilute solutions of poly(methyl methacrylate) below the theta temperature. *Polymer Journal* **2014**, *46*, 641-645.

43. Emerson, J. A.; Toolan, D. T. W.; Howse, J. R.; Furst, E. M.; Epps, T. H., Determination of solvent-polymer and polymer-polymer flory-huggins interaction parameters for poly(3-hexylthiophene) via solvent vapor swelling. *Macromolecules* **2013**, *46*, 6533-6540.

44. Tung, Y. C.; Wu, W. C.; Chen, W. C., Morphological transformation and photophysical properties of rod-coil poly[2,7-(9,9- Dihexylfluorene)]-block-poly(acrylic acid) in solution. *Macromolecular Rapid Communications* **2006**, *27*, 1838-1844.

45. Jaczewska, J.; Raptis, I.; Budkowski, A.; Goustouridis, D.; Raczkowska, J.; Sanopoulou, M.; Pamuła, E.; Bernasik, A.; Rysz, J., Swelling of poly(3-alkylthiophene) films exposed to solvent vapors and humidity: Evaluation of solubility parameters. *Synthetic Metals* **2007**, *157*, 726-732.

46. Fytas, G.; Nothofer, H. G.; Scherf, U.; Vlassopoulos, D.; Meier, G., Structure and dynamics of nondilute polyfluorene solutions. *Macromolecules* **2002**, *35*, 481-488.

47. Lemaury, V.; Cornil, J.; Lazzaroni, R.; Sirringhaus, H.; Beljonne, D.; Olivier, Y., Resilience to Conformational Fluctuations Controls Energetic Disorder in Conjugated Polymer Materials: Insights from Atomistic Simulations. *Chemistry of Materials* **2019**, *31*, 6889-6899.

For Table of Contents Only

